HELSINKI UNIVERSITY OF TECHNOLOGY
Department of Electrical and Communications Engineering

Clemens Icheln

CHARACTERISATION OF RF RADIATION PROPERTIES OF SMALL EQUIPMENT

This thesis was submitted in partial fulfilment of the requirements for the degree of Licentiate in Technology,

Supervisor
Professor Pertti Vainikainen

2nd evaluator
Dr. Sci. (Tech.) Anssi Toropainen

Preface

The work on which this thesis is based was carried out at the Institute of Radio Communications / Radio Laboratory of Helsinki University of Technology. It has been mainly funded by TEKES and the Academy of Finland. I also received financial support from the Wihuri foundation. I would like to thank all these institutions, and the Radio Laboratory, for making this work possible for me.

I am especially thankful for the many ideas and helpful guidance that I got from my supervisor professor Pertti Vainikainen during all my work. To Anssi Toropainen also thanks for his time for discussions and many useful comments.

Of course I would also like to thank the staff of the Radio Laboratory, which provided a pleasant and inspiring working atmosphere, in which I got lots of help from my colleagues - let me mention especially Tommi, Jani, Annemarie, Lorenz and Lauri - without whom this work would not have been possible.

And finally I want to say thanks for the encouragement I got from my parents during the last years.

Espoo, October 24, 1999,

Clemens Icheln

HELSINKI UNIVERSITY OF TECHNOLOGY

Abstract of the Licentiate Thesis

Author:	Clemens Icheln	
Name of the thesis:	Characterisation of RF radiation properties of small equipment	
Date:	24.10.99	**Number of pages:** 35
Department:	Department of Electrical and Communications Engineering	
Professorship:	Radio Engineering	
Supervisor:	Professor Pertti Vainikainen	
2nd evaluator:	Dr. Sci. (Tech.) Anssi Toropainen	

In this work new methods for the characterisation of the RF radiation properties of different small devices have been investigated. The first two parts of the work relate to the measurements of small antennas as used in mobile communication systems. The aim is to provide an alternative measurement environment to large, fully anechoic chambers in the special case of *small* antenna calibrations. The use of small chambers such as GTEM cells and small anechoic chambers is proposed. Both options have been constructed and investigated by both simulations and measurements. The results show the usefulness of a GTEM cell in measuring radiation properties such as 3-dB bandwidth and total radiated power of small, moderately directive antennas. The results indicate also, that a small anechoic chamber can be used for measurements of 3D radiation pattern and directivity of small antennas, with the same uncertainty as in large chambers. Furthermore, the influence of the feeding cables attached to the radiation of a small antenna under test has been reduced by a novel method which suppresses the propagation of leakage and parasitic currents on the surface of the feeding cable.

The third part of the work concentrates on the definition of radiated EMI pre-compliance tests, carried out during the design phase of a new equipment by means of computer simulations. Hereby, passing the final EMC tests shall be ensured, or the probability of compliance increased. One Finite Element Method tool and one Method of Moments tool have been applied to two different test cases consisting of switched mode power supplies, to predict their radiation. The results have been compared to GTEM cell radiation measurements, and they show sufficient agreement to prove the usefulness of computer simulations for EMI prediction.

Keywords: Small antenna measurement, mobile communications antennas, anechoic chamber, GTEM cell, Electromagnetic Compatibility (EMC), computer 3D-field simulation, radiated electromagnetic interference (EMI), pre-compliance test.

List of Publications

This thesis is based on the work contained in the following papers:

[P1] C. Icheln, P. Haapala, P. Vainikainen, 'Application of a GTEM cell to small antenna measurements', *Proceedings of the 1997 IEEE AP-S International Symposium and URSI North American Radio Science Meeting*, Montreal, Canada, July, 1997, pp. 546 - 549.

[P2] C. Icheln, J. Ollikainen, P. Vainikainen, 'The Effects of RF Absorbers on Measurements of Small Antennas in Small Anechoic Chambers', *Proceedings of the IEEE Instrumentation and Measurement Technology Conference*, Venice, Italy, May, 1999, pp. 209 - 212.

[P3] C. Icheln, J. Ollikainen, P. Vainikainen, 'The Effect of RF Absorbers in the Vicinity of Small Antennas', accepted for publication in *Microwave and Optical Technology Letters*, Vol. 22, No. 5, September 5, 1999, 3 pages.

[P4] C. Icheln, J. Ollikainen, P. Vainikainen, 'Reducing the influence of feed cables on small antenna measurements', accepted for publication in *Electronics Letters* in June 1999, 2 pages.

[P5] C. Icheln, T. Laitinen, M. Sippola, H. Siren, R. Sepponen, P. Vainikainen, 'Computer simulations and near field measurements for the prediction of radiated EMI', *Proceedings of the IEEE 1998 International Symposium on Electromagnetic Compatibility*, Denver, USA, August, 1998, pp. 878 - 881.

In the case of paper [P1] this author had the main responsibility in preparing the paper and conducting the measurements presented in the paper. Papers [P2] and [P3] were again mainly prepared by this author. In those papers the author got assistance during the measurements from the co-author J. Ollikainen who also provided the antennas that were measured. The main idea presented in paper [P4] was a joint idea of all the authors while the main responsibility of the paper was with the main author. Paper [P5] is a joint publication of the authors. This author was responsible for the part of the paper that deals with computer simulations, in which he got assistance from the co-authors M. Sippola and H. Siren.

Contents of summary of Licentiate Thesis

1. Introduction

The determination of the direction and frequency dependent RF radiation characteristics of small radiating devices is an important research subject in the field of radio engineering. E.g. in the area of future mobile communication systems the behaviour of antennas in their working environment is usually characterised by the three-dimensional radiation pattern, gain, radiation efficiency and bandwidth with respect to a given maximum return loss at the input of the antenna. Measurements during the design of new small antennas for the use in mobile handsets and the final calibration of those antennas requires an environment with a well-defined electromagnetic field strength at the position of the antenna under test (AUT). A typical frequency range of current and nearest future mobile communications systems is from around 0.9 GHz to 5 GHz.

To excite a well-defined field, typically a calibrated electromagnetic field source is placed in an environment without reflections from surrounding objects. A fully anechoic chamber (FAC) is such a so-called free-space measurement environment, in which all walls are completely covered by absorbing material, and no conducting surfaces are present. In anechoic chambers one can reach field homogeneity of ± 0.5 dB, which is required by antenna calibration standards [1, pp. 19-20], or even down to ± 0.1 dB. Consequently, in order to determine the radiation characteristics of small antennas accurately, measurements are typically performed in anechoic chambers. Hereby, the measurement of the directly transmitted electromagnetic field is possible without considerable interferences from reflected fields.

The absorber lining is the main part of the installation costs of anechoic chambers. A typical distance between the AUT/EUT and the measurement antenna is 3 – 5 m, or even more. Distances between the antennas and the side- and backwalls, as well as to the floor and ceiling, are typically 1 – 3 m. The dimensions of anechoic chambers are therefore quite impressive, leading to substantial costs. When performing measurements of small antennas for mobile communication systems alternatives with much smaller dimensions and hence lower installation costs seem preferable. Therefore, one goal of this thesis is to investigate the feasibility of using small chamber in antenna measurements and to find the limits for their use in terms of dimensions, frequency range and measurements uncertainties.

Chapters 2 and 3 deal with the application of smaller chambers like the Gigahertz Transverse Electromagnetic Mode (GTEM) cell and especially small fully anechoic chambers to small antenna measurements. In Chapter 2 the applicability of the GTEM to small antenna measurements with certain restrictions is verified by several measurements of small antennas. Chapter 3 relates to the feasibility of decreasing the size of small anechoic chambers to table-top size by bringing measurement antenna and AUT, as well as sidewalls and AUT very close to another. In Section 3.4 special attention is paid to the problem of measurement cables attached to small antennas or mobile handsets, which cause changes in the radiation characteristics of the AUT. A simple solution how to minimise the errors is proposed.

Another common case where the radiation characteristics of small devices are measured are tests for radiated electromagnetic interference (radiated EMI) of electronic equipment. The measurement set-up and the field uncertainty requirements are slightly different to those used in antenna calibrations. Instead of a full 3-dimensional antenna pattern with complex field strength and two polarisations, electromagnetic compatibility standards just set a limit for the maximum total field strength at 3 m or 10 m distance. During tests for radiated EMC the EUT is basically rotated around a vertical axis and the maximum field strength is recorded at one or several heights [2]. Furthermore, while antennas in mobile communications are typically narrowband devices, EMC tests are performed over several octaves, i.e. from 30 MHz to 1 GHz, although nowadays a limit up to 2 GHz seems preferable and is under discussion.

Standard tests of the radiated EMC are performed on an Open Area Test Site (OATS), where a semi free-space environment is created by allowing the EUT or measurement antenna to radiate into the atmosphere, while the floor of the measurement site works as a conducting ground plane. A measurement antenna that picks up the field excited by the EUT is situated at a distance of 10 m from the EUT that is rotated around a vertical axis. A height scan between 1 m and 4 m is performed to find the maximum of the interference of direct and reflected field [3, pp. 51-56]. Requirements for the field strength uncertainty at the position of the EUT lie within ± 4 dB. Although these test sites are less cost intensive to construct than fully anechoic chambers, they have disadvantages such as the exposure of such test environments to surrounding sources of electromagnetic waves, e.g. public radio stations and mobile communication systems. Therefore in future standards the optional use of anechoic chambers for EMC test will be implemented [4].

An alternative closed chamber that is nowadays used in standard EMC tests is the GTEM cell [2], [5], [6], [7]. It is basically a widened, asymmetric, stripline with a very wideband matched termination. During susceptibility measurements in a GTEM cell an EUT is exposed to a vertically polarised electrical field. During radiated immunity tests the EUT couples its radiated energy into the GTEM cell and the output power at the port of the cell is measured. By characterising the EUT by electric and magnetic multipoles, the measurement can be accurately correlated to standard OATS measurements. GTEM cell measurements involve no secondary antennas, and the installation costs are much lower compared to an OATS or FAC.

However, tests in GTEM cells are not as generally applicable to larger EUTs, as are tests in large, conventional test environments. This is due to the limited size of GTEM cells and the sensitivity of the field-strength homogeneity in the GTEM cell to dielectric or conducting material placed in the test volume. The field strength in the test volume is basically defined by the voltage and distance between inner and outer conductor. The effective distance is altered by a large conducting object which affects the field strength homogeneity much stronger than on an OATS where generally far field conditions are valid at the position of the EUT.

In order to fulfil the field homogeneity requirements an EUT in a GTEM cell can not be larger than 1/3 of the height between the centre conductor and the floor. This clearly limits the size of equipment that can be tested in a moderately sized GTEM cell. For the same reason, the use of automated positioner systems introduces more problems than on a large OATS, as well as

the power supply to the EUT. Cables leading to the testing volume tend to affect the fields measured at the position of the EUT considerably.

Even though the GTEM cell offers a considerably less costly and time consuming method for EMI measurements, it is still a considerable cost and time factor during the assessment of the radiated EMI of electrical equipment, and is thus a method that is used e.g. as a last test before sending the equipment to the final, accredited EMC test laboratory. In order to get preliminary knowledge of the radiation properties of e.g. a new equipment during its design, it seems preferable to obtain this knowledge without any time consuming and expensive measurements. Therefore, the second goal of this thesis is to prove the feasibility of computer EM field simulations for predicting radiated EMI of small equipment. Those methods are investigated in Chapter 4. Procedures for two commercial software packages involving the Finite Element Method and the Method of Moment have been developed, described and evaluated for two test cases consisting of switched mode power supplies. When comparing the results to GTEM cell radiation measurements, they show sufficient agreement to prove the feasibility of computer simulations for EMI prediction of small equipment.

2. GTEM cell and small antenna measurements

In EMC measurements the GTEM cell is accepted as a sufficient tool for radiated susceptibility tests as well as for measurements of radiated emissions. From this the idea arose to use the GTEM cell to characterise small antennas. This is however not an obvious procedure, as the requirements for the field homogeneity in EMC test measurements are less stringent (± 3 – 4 dB) than in antenna measurements (± 0.1 – 0.5 dB). Furthermore, one would expect a strong influence of the metal cell walls on the radiation characteristics of the antenna, as well as - possibly multiple - reflections which would affect the measured radiation pattern. In [8] and [9] was shown that these effects are negligible in a conventional TEM cell. According to [10] the gain of an antenna can be measured in a GTEM cell with an average accuracy of better than ± 1 dB. All three articles also mention that reciprocity is fulfilled, i.e., the antenna under test may be used as the transmitter or receiver without changing the result. So in the first part of this research work the possible application of a GTEM cell to small antenna measurements was more thoroughly evaluated. Test measurements of radiation patterns with several small antennas were carried out and compared to reference measurements. Field probe measurements were used to analyse the field properties inside the GTEM cell.

2.1. Measurements of field patterns of moderately directive narrow-band patch antennas

The radiation patterns of three small patch antennas and a small helix antenna were measured at frequencies between 0.9 and 3.8 GHz. The set-up of the antenna measurement inside the GTEM cell is described in Figure 1. In all cases a good correspondence between the GTEM cell and anechoic room measurements was seen in the main lobe pattern [P1]. Thereby e.g. the 3-dB bandwidth of the antennas could be determined quite accurately. However, the minima and the back lobe region suffered from the limited dynamic range of the cell, i.e. a front to back lobe ratio of only 20 dB could be measured. The power reflection coefficient of the termination of the cell is about −20 dB. So, when the main lobe is directed towards the back of the cell, and the directivity of the antenna is in the area of 20 dB or more, the interference between direct and reflected field is dominant and the information about the back lobe level can not be recovered.

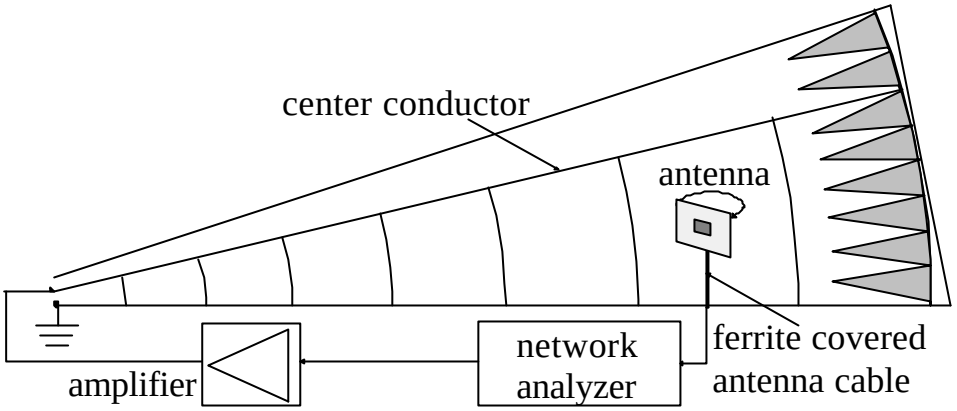

Figure 1: Antenna measurement set-up inside GTEM cell

2.2. Measurements of antennas with special characteristics in their radiation pattern

The results obtained in the measurements with a modified patch antenna that contained two parallel parasitic patches proved the good isolation of the GTEM cell between co- and cross-polarisation, which is an important factor in measurements of mobile phone antennas. The parasitic patch of the antenna caused the radiation to turn the polarisation as a function of frequency. The band in which the polarisation was horizontal instead of vertical could clearly be determined in the GTEM cell (see Figure 2). The measurements in the GTEM cell and in a FAC were made comparable by doing a parallel reference measurement with a monopole probe in both GTEM cell and anechoic chamber. The difference of the two curves obtained from the monopole in GTEM cell and FAC, was added to the patch antenna curve that was measured in the GTEM. Hereby, the frequency response of the GTEM cell was calibrated.

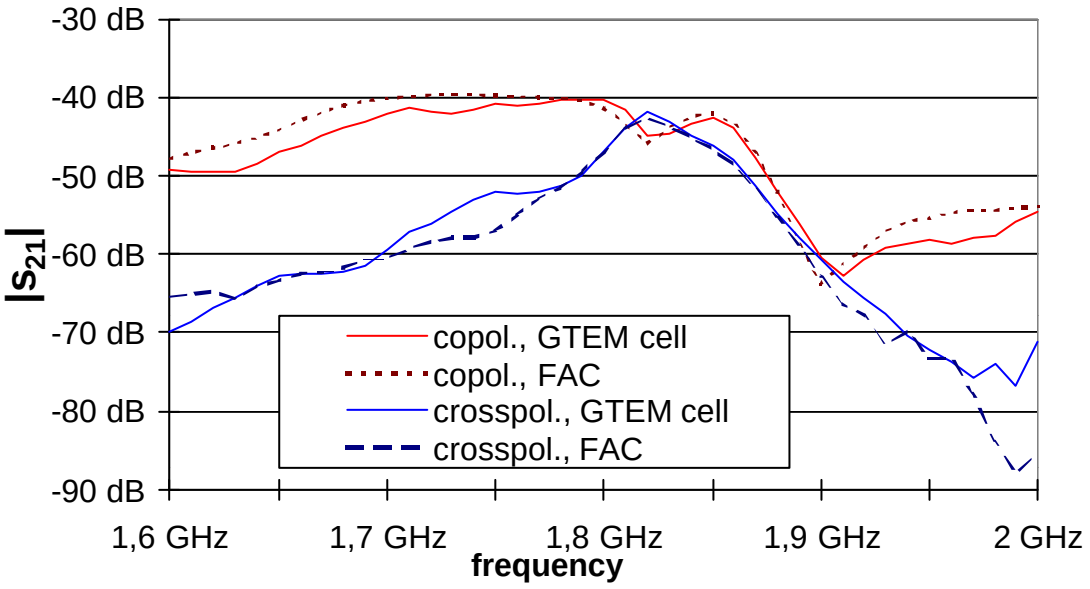

Figure 2: Comparison of the copolarised and crosspolarised E-field of the triple-patch antenna in the GTEM cell (solid) and in the anechoic room of IRC (dotted, dashed).

2.3. Field uniformity in the testing volume at frequencies above 1 GHz

The field homogeneity of an antenna test site is an important factor in the evaluation of a measurement site. Therefore, measurements of the field homogeneity in the testing volume of the 2.1 m long GTEM cell at IRC were performed. The vertical field strength at the centre of the testing volume and the field strength at positions towards the side walls of the cell were compared (see Fig. 3). An increasing field inhomogeneity of more than ±1 dB was discovered at frequencies > 2 GHz (Fig. 4).

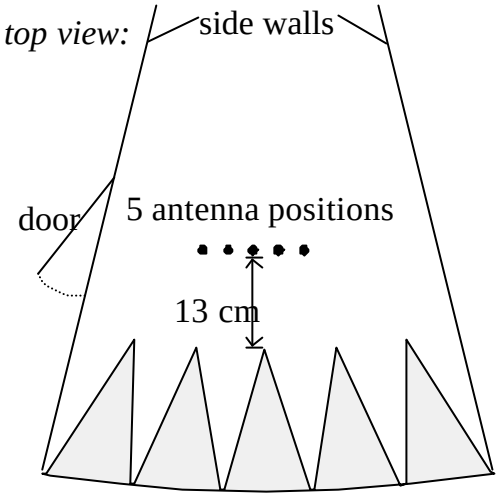

Figure 3: Measurement set-up when determining the field homogeneity inside the test volume of the GTEM cell.

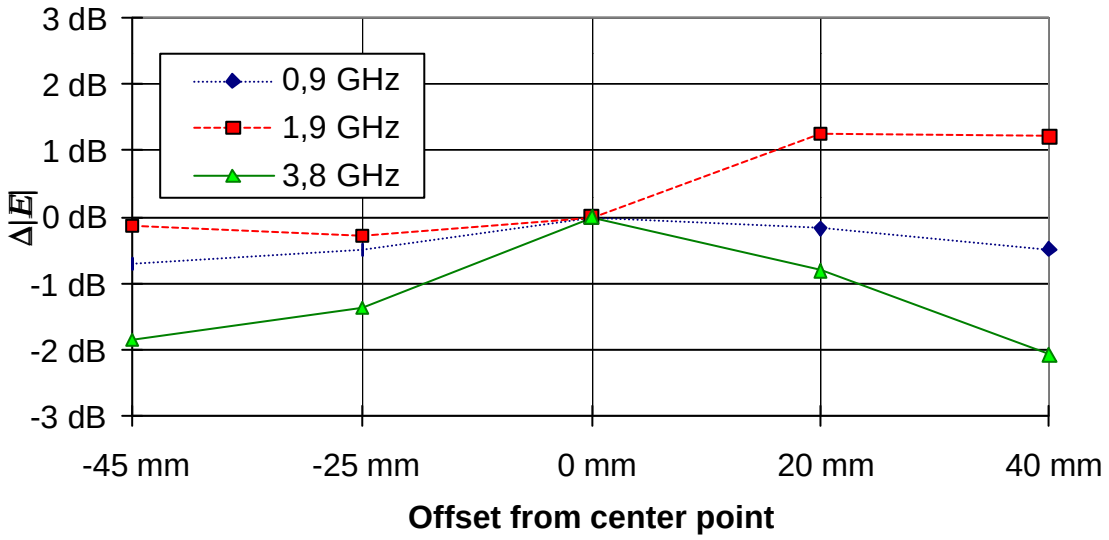

Figure 4: Electric field variations along a line perpendicular to the longitudinal axis of the GTEM cell. At each frequency the field strength was normalised to the centre point of the test volume.

Reflections from the termination of the cell, as well as higher order modes excited by the objects inside the GTEM cell [11], are reasons for the field fluctuations in the testing area. In the GTEM cell used in these measurements the test volume is situated 1.3 m from the input port of the cell. At this position the height between center conductor and bottom wall is 390 mm. In this case, at 1 GHz theoretically $^1/_3$ of the power in the testing volume propagates in higher order waveguide modes (see Fig. 5). These higher order modes cause a deterioration in the field homogeneity inside the testing volume of the GTEM cell. When the antenna is the transmitter, the position of the antenna has an influence on which higher order modes are excited. In the case of a patch antenna this means that different areas of the antenna surface may actually couple to different modes. Furthermore, the higher order modes cannot propagate all the way to the input port of the cell, as the decreasing cross sectional dimensions of the waveguide raise the cut-off frequency continuously until only the TEM mode can propagate further. The energy is partly transferred back into lower modes and finally reaches the port in the TEM mode, or it is reflected back towards the termination of the cell. This loss of energy that is not measured at the port of the cell affects the measurements. The amount of energy in the cell that may be propagating in higher order modes increases with the frequency. This fact limits the useful frequency range for the aspired application of the GTEM cell.

At 0.9 GHz the measured field homogeneity seen in Fig. 3 is good enough for the measurements of small e.g. patch antennas or complete mobile handsets. For such small antennas one can furthermore expect a directivity less than 20 dB so the limited dynamic range of the cell discussed above is not an obstacle. However, with an increased field inhomogeneity in the cell and a more directive behaviour of a small antenna, measurements at 1.9 GHz have to be analysed carefully, and above 2 GHz the 2.1 m long GTEM cell does not appear to be a suitable device for antenna measurements. This fact is not likely to change with a different size of the GTEM cell. A larger cross section will only increase the probability of higher order modes, while a smaller cross section will impose a too small limit to the size of the measurable antenna. As a point of reference, the testing volume inside the 2.1 m long GTEM cell is about 130 mm high and a typical mobile handset is about 100 - 130 mm long.

At frequencies below 0.9 GHz, where e.g. some pager systems operate, one can expect the field homogeneity inside the GTEM cell not to be distorted more than seen at 0.9 GHz. Rather in the opposite, as the cut-off frequencies of the higher order modes are beyond these low frequencies. However, at lower frequencies the quality of the wideband termination has to be taken into consideration, because the radiation termination by the RF absorbers becomes less effective at lower frequencies. This effect can be expected to be considerable only below 400 -500 MHz for cases where medium sized or large RF absorbers are used for the termination [12]. So, already a medium sized GTEM is a useful tool for antenna measurements from about 400 – 2000 MHz.

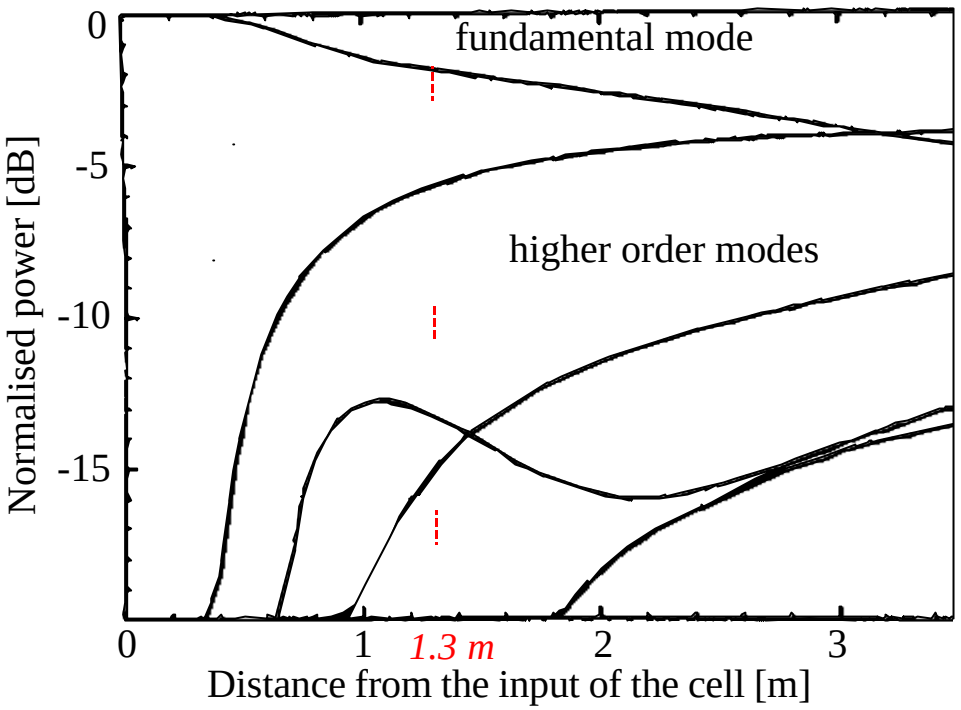

Figure 5: Power distribution in fundamental and higher order modes in a GTEM cell at 1 GHz [11].

2.4. Antenna efficiency measurements in a GTEM cell

The accurate efficiency of an antenna is rather difficult to obtain with conventional measurement methods. Especially in the case of mobile handset antenna the conventional Wheeler Cap method does not allow to measure the efficiency of a handset together with a human head model. The size of the radiating object must be small enough to fit into the cap which again is sizewise limited by the first cavity resonance. Also the inclusion of a lossy body like the head model would violate the idea of the Wheeler Cap.

Alternatively, during the last years reverberating chambers have been increasingly used for efficiency measurements [13]. As opposed to the Wheeler Cap the principle of reverberating chambers builds on the existence of cavity resonances as a means of averaging the radiated power. Therefore the chamber and the AUT are not limited in size. However, the inclusion of lossy material in the measured object is not unproblematic, as the resonances change and thus the calibration of the empty cell becomes inaccurate. The use of waveguides for efficiency measurements was proposed in [14] presenting two new methods. In both methods the small antenna is placed inside a relatively small waveguide. Furthermore, the use of TEM cells for total radiated power measurements has been presented in [15]. Generally, the use of waveguides overcomes the limitation of the Wheeler Cap method in terms of size of the antenna, as well as the limitation of the reverberating chamber in terms of including lossy material. This is due to the fact that waveguide measurements rely on actually measuring the radiation itself. Even if it involves the time consuming measurement of the 3D radiation pattern, the use of GTEM cells in efficiency measurements seems like a very promising alternative for efficiency measurements.

3. Small anechoic chambers and the characterisation of small antennas and mobile handsets

In the second part of this thesis, the feasibility of drastically decreasing the dimensions of anechoic chambers, for the use of small antenna measurements at 1−2 GHz, was investigated. Table-top sized anechoic chambers can be implemented in a straight-forward manner at higher frequencies, e.g. at several GHz, where the wavelength is only of the order of 10 − 50 mm. Such a small anechoic chamber, even movable, was designed. e.g. in [16]. With dimensions of only $2.25 \times 1.2 \times 1.2$ m^3, the chamber that was designed for the frequency range above 18 GHz showed good results. However, at RF frequencies with wavelengths of 100 − 500 mm the feasibility of such a small chamber is not obvious. The reasons for that are discussed in the following.

3.1. Effect of the small distance between the antennas

The minimum possible distance between the AUT and the measurement antenna is an important factor that will yield a lower limit for the size of an anechoic chamber. This minimum measurement distance depends on several factors.

First of all a certain minimum desired ratio between the far field and the near field of the AUT should be defined. This ratio can be calculated e.g. for a single electric dipole directly as a function of distance. The vertical electric field excited by an electric dipole

$$E_q = K_E \cdot \sin\theta \cdot \left| \frac{j}{kr} + \frac{1}{k^2 r^2} - \frac{j}{k^3 r^3} \right| \qquad (1)$$

[17, p.135] at a distance r, where $K_E = IL\eta k^2 (4\pi)^{-1} e^{-jkr}$, with the current I on the dipole of length L, the free-space wave impedance $\eta = 120\pi$, and the wave number $k = 2\pi f/c_0$.

One can then estimate for the case of a small antenna the minimum measurement distance that is necessary to reach a certain dominance of the far field. By assuring that the measurements are proper far-field measurements one will not have to perform near field to far field transformations.

The small radiator can be described with a combination of complex-excitation electric and magnetic dipoles with random orientation. Due to the random orientation the near-field terms, i.e. the $1/k^2r^2$ and the $1/k^3r^3$ terms, in Eq. (1) can be in phase with the far-field term. Now the worst-case relative error in the assumed far field due to the near field at the position of the measurement antenna can be estimated to be

$$e_{rel} = \frac{\left|\frac{1}{kr}\right|}{\left|\frac{1}{kr} + \frac{1}{k^2 r^2} + \frac{1}{k^3 r^3}\right|}. \qquad (2)$$

At 900 MHz and a measurement distance of 1 m Eq. (2) yields an error of 5.6% or ±0.47 dB which will have to be taken into account for the estimation of the total measurement error. At a distance of 0.5 m the near-field error is almost 1 dB which would be a generally unacceptable error margin for antenna calibrations. For comparison, the near-field error at 5 m distance is <0.1 dB. At 1.8 GHz the error at 1 m decreases down to 0.22 dB, and at 5 m measurement distance it would even be smaller than 0.05 dB (see Table 1).

Table 1: Possible inaccuracy due to far field assumption, at 900 MHz and 1.8 GHz.

frequency	d = 5 m	d = 1 m	d = 0.5 m
900 MHz	±0.093 dB	±0.47 dB	±0.96 dB
1.8 GHz	±0.043 dB	±0.022 dB	±0.44 dB

Not only the influence of the assumed far-field condition in the transversal field, but also the influence of the radial field component of the near field

$$E_r = 2K_E \cdot \cos\vartheta \cdot \left|\frac{1}{k^2 r^2} - \frac{j}{k^3 r^3}\right| \qquad (3)$$

[17, p.135] has to be taken into account. The radial field (3) reaches its maximum at that angle (namely at $\vartheta = 0$) where the transversal component has its minimum. Therefore, the radial near field might influence the detection of the nulls of the radiation pattern of an antenna. At 900 MHz and 1 m distance the maximum level of the radial component is 19.5 dB below the maximum level of the transversal component.

Most antennas that are used as measurement antennas have very good polarisation purity between transversal and radial fields. In case of a horn antenna, it is still possible that a small portion of the radial field couples into the antenna especially at the edges of the aperture where the radial field produces a small vertical field component in the aperture. However, the power distribution of the electric fields across the aperture of the horn does not support that waveguide mode and attenuates it. At the feed of the horn only the far-field part of the coupled fields is left to be detected.

The measurement antenna is likely to be a larger antenna, e.g. a horn antenna with a certain aperture. If a spherical wave is assumed to propagate from the AUT, the flat aperture of the measurement antenna will be illuminated by wave fronts with different phases in the centre and the corners of the aperture (see Fig. 6). This phase error is investigated in the following, for the case of a wideband corrugated horn antenna with an aperture of 245 × 142 mm^2.

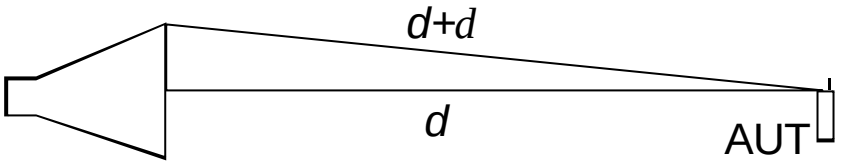

Figure 6: The aperture of the measurement antenna is illuminated by wave fronts with a phase difference of d / l .

Seen from the AUT, the different areas of the horn antenna aperture - like centre and corners of the waveguide - are effectively situated at different distances. Depending on the distance between the two antennas, the phase error and amplitude error due to this inconsistent distance is significant or negligible. According to [18] distances smaller than $D^2/4l$ are considered to be in the Fresnel region which is characterised by a strong reactive near-field effect. D denotes the maximum dimension of the antenna. In fact, different sources in literature define the Fresnel zone differently. E.g. according to [19, p. 60, pp. 809-810] $2D^2/l$ denotes the sphere that forms the border between the Fresnel zone and the so-called Fraunhofer region in which far-field conditions are valid. This means at 900 MHz and with the horn antenna with an aperture of 245×142 mm^2 the Fresnel zone limit is 26 mm according to T. Macnamara and 211 mm according to J. D. Kraus. Apparently, the near-field conditions do not stop abruptly to be valid, as little as the far-field conditions are abruptly valid beyond this border sphere. Rather one should think of a border area between Fresnel and Fraunhofer regions, within which far-field conditions may be assumed with a certain error margin which has to be taken into account.

It was calculated that for distances larger than $4D^2/l = 422$ mm for the same antenna we can expect the ratio of the measured gain to the gain at an infinite distance to be about 0.99 [18], i.e., an inaccuracy of 1% which is acceptable for a gain measurement. Another effect of phase variations along the aperture of the measurement antenna is, that nulls in the radiation pattern are partially filled. In Fig. 7 the effect is illustrated for distances $2D^2/l$, $4D^2/l$ and an infinite difference [1, p.21]. At these distances the phase error is 22.5° and 11.25°, respectively. Small antennas generally do not show a strong directivity and the exact position of nulls or the exact level of side-lobes below 20 dB are usually not very important in mobile handsets, so to set the limit for the measurement distance at $d > 4D^2/l$ is perfectly sufficient.

It should be noted that also the AUT may cause phase errors. Even if small mobile handsets should obviously be rotated around the feed point of the antenna, the handset is not a symmetric dipole like a monopole on an infinite ground plane. It is rather an asymmetric dipole along which the phase centre may vary as a function of frequency around the feed point of the antenna. In the case of small distances between the AUT and the measurement antenna, changes in the location of the phase centre during the rotation of the AUT cause considerable variations in the measurement distance. The knowledge of the accurate distance is an important factor in the calibration, because the path loss between the two antennas determines the correction coefficient for the transmission coefficient when measuring the gain of the AUT.

At 5 m measurement distance the deviation in the phase centre is usually neglected. This is reasonable, as the phase centre only varies within the dimensions of the antenna and a possible phone chassis. The length of modern mobile handsets is around 80 mm - 100 mm without the

antenna. As the field strength E [dB] is proportional to 20 log d, the displacement of the phase centre along the chassis to e.g. 50 mm from the antenna can lead to a worst case inaccuracy in the field strength of about 1% i.e. less than ± 0.09 dB. However, when measuring the same mobile handset at e.g. 0.5 m, the changing phase centre could cause a relative error in distance of up to 10%, i.e. a field inaccuracy of ± 1 dB, which would be unacceptable for antenna calibrations.

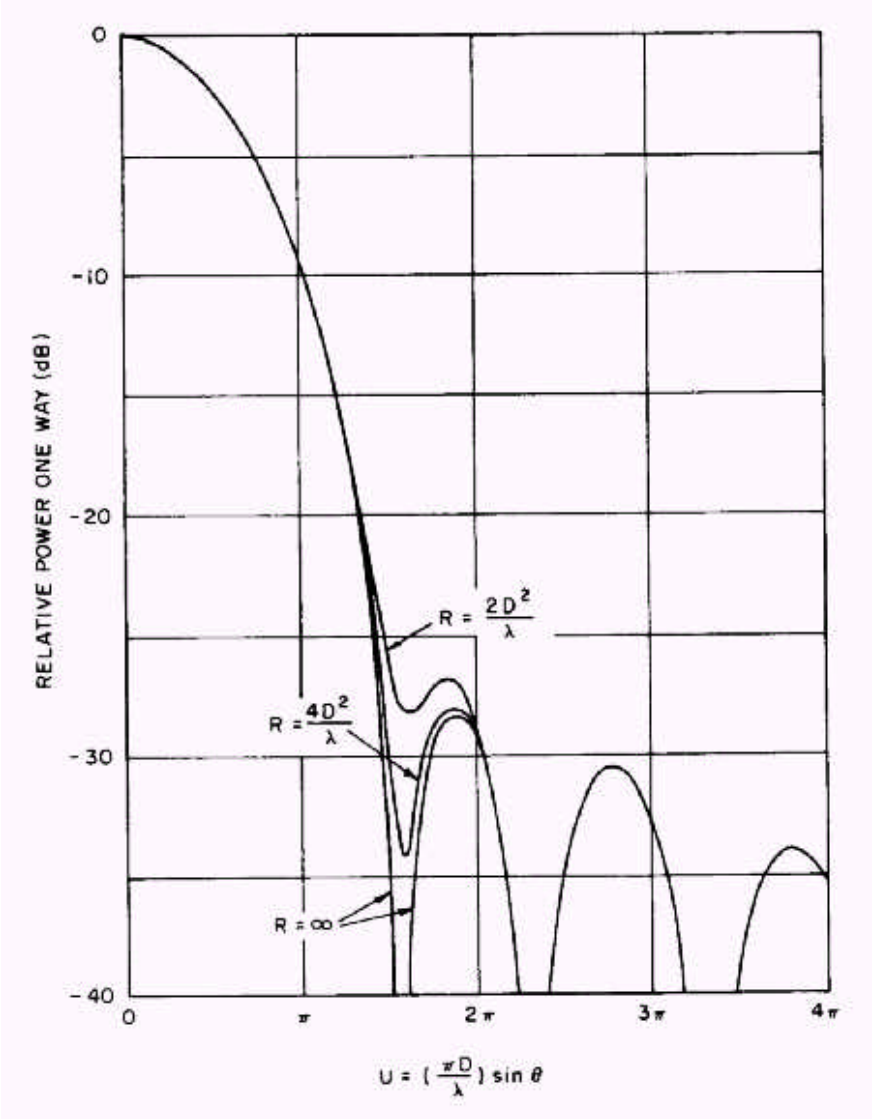

Figure 7: Calculated radiation patterns illustrating the effect of phase errors encountered in measuring patterns at the ranges indicated [20, pp. 14-10].

At a distance of 1 m between the antennas and making the optimistic assumption that the actual displacement of the phase centre from the feed point of the antenna may be about 10 mm, the relative distance error causes acceptable inaccuracy in the measured amplitude of the E-field of ± 0.09 dB. It has to be noted, that the phase centre of the radiation can be expected to be situated close to the feed point of the antenna, i.e. at one end of the handset. So in order to reach the above calculated relative distance error at 1 m distance one has to make sure the rotation is actually performed around the feed point of the antenna and not around the physical centre of the handset.

The position of the phase centre is much more difficult to reconstruct, when the measured AUT is placed in the anechoic chamber together with a human head model. This is done to take into account the influence of the user on the efficiency and radiation pattern of the handset during operation. The head model represents basically a relatively large, round and lossy body. Even if it therefore does not resemble a secondary radiator or a dielectric lens, it may still work as a small reflector at the frequencies that are discussed here (i.e. > 900 MHz). The antenna of a handset in operation is usually situated about 20 – 30 mm from the head of the user. The effective phase centre of the antenna-reflector combination may be anywhere between these points, i.e. up to about 30 mm from the feed point of the antenna. Then the above mentioned displacement of the phase centre by only 10 mm may not be valid anymore. Instead, one has to expect the inaccuracy due to the variance in the phase centre position to be around ± 0.1 – 0.26 dB (see Table 2).

Table 2: Field strength inaccuracy in case of displacement of the phase centre from the antenna feed point, *d* = measurement distance.

Displacement	d = 5 m	d = 1 m	d = 0.5 m
10 mm	±0.02 dB	±0.09 dB	±0.18 dB
30 mm	±0.05 dB	±0.26 dB	±0.54 dB

As a last point the influence of multiple reflections between the apertures of the two antennas may have to be taken into account [1, p. 17]. In mobile communications systems, resonant type antennas are used, such as helix or patch antennas. At resonance such an antenna transforms most of the incoming radiated energy into an electric signal at its port, and vice versa. However, the antenna still reflects or scatters some part of the incident wave. At smaller distances d between the antennas the transmitting antenna will cover a greater solid angle seen from the receiving antenna, i.e. it is exposed to more of the scattered field reflected back from the receiving antenna than for a larger distance. Also the free-space attenuation of the scattered fields at distance d is smaller than for conservative measurement distances of several meters. So, when two antennas face each other at 1 m, those multiple reflections might not simply be neglected as is done for larger measurement distances and have to be investigated.

The aperture of the horn antenna described above is A_1 = 3500 mm^2 and the worst case aperture of a small radiator can be estimated to be in the range of A_2 = 500 mm^2. The back scattering from the antenna aperture in both cases is assumed to be around 50 %, i.e. $r_1 = r_2 = 0.5$. The scattered fields can be assumed to propagate spherically from the antenna apertures and thus the scattered power density at a distance d is $1/4\pi d^2$. The ratio of the power P_{in} that is directly received by one of the antennas and the power P_{rr} that is reflected twice (once from the receiving antenna and then back from the transmitting antenna) can be estimated as

$$\frac{P_{rr}}{P_{in}} = \frac{r_1 A_1 \cdot r_2 A_2}{(4\pi d^2)^2} \approx -75 \text{ dB}. \qquad (4)$$

where d = 1 m measurement distance. This very low interference level can be neglected during antenna measurements.

As a final conclusion it can be said, that of all error sources that are related to the small distance between the antennas, the assumption of far-field conditions introduces the largest inaccuracy to the antenna measurements, as it is almost ± 0.5 dB at 900 MHz and 1 m measurement distance. For 1.8 GHz this effect is again negligible, however, when a head model is included in the antenna measurements of mobile handsets, the unknown exact position of the phase centre may contribute up to ± 0.26 dB inaccuracy in the measured field strength at 1 m measurement distance.

3.2. Effect of RF absorbers in the vicinity of small antennas

Another limiting factor for decreasing the size of a small anechoic chamber is the distance between the absorbers and the AUT. The distance between the antennas can not be decreased arbitrarily for two reasons. At a too short distance the carbon loaded foam will be situated in the reactive near field of the antenna, whereby the current distribution on the antenna and also on the chassis may change, and hence the whole radiation pattern of the handset might change. The second reason is that when the distance between antenna and side walls decreases, the incidence at the side walls between the antennas becomes increasingly grazing. At such non-normal incidence the reflection coefficient of the absorbers gets poorer. Hence, a stronger interference pattern between direct and reflected field is caused which affects the measured radiation pattern. In [P2] and [P3] these two effects were investigated by both measurements and computer simulations. It was found that absorbers with the length of 610 mm do not have any measurable effect on the radiation characteristics of a small antenna at around 1.8 GHz, as long as the distance between the AUT and the absorbers is more than 100 mm. Furthermore the transmission channel formed by the absorbers between the antennas must be wider than 100 mm in order to have an undisturbed transmission between the AUT and the measurement antenna. The work has also proven, that computer simulations are a useful tool for the field analysis and design of small anechoic chambers.

3.3. Design, construction, and performance of a small shielded anechoic chamber

The present work includes the construction and investigation of a small anechoic chamber in which the measurement distance between the AUT and the measurement antenna is decreased to 1 m. The distance between the AUT and the absorbers on the side- and backwalls is reduced to 200 mm. By using such small or even smaller anechoic chambers it would be possible to perform quick measurements of small antenna characteristics in decentralised, or eventually even portable, table-top sized measurements environments situated close to the developers of new antennas. Hereby, faster assessment of the behaviour of the mobile handset in operation would be possible.

The size of the absorbers is determined by the requirements for the reflectivity level of the anechoic room. This again is dependent on the gain of the antennas involved, i.e. the measurement antenna and the AUT. Usually a horn antenna is used as a measurement antenna. In the following an average value of 8 dB for the gain of a horn antenna, and 2 dB for the general case of a AUT are used. The size of the AUT determines the size of the test volume in which the reflectivity level has to be met. For a 20 mm long antenna on a 100 mm long chassis, which has to be rotated around the feed point of the antenna, a test volume with a diameter of 250 mm is sufficient and will be used in the following.

In the Radio Laboratory a chamber was built with a size of 2.5 m by 2.5 m and a height of 2.40 m (Figure 8 (l.)). Relatively large absorbers were used in this chamber (Figure 9). These absorbers were needed because the chamber is also meant for EMC radiated emissions near-field measurements down to 30 MHz. The specifications for a test volume with a diameter of 250 mm were given as follows: ± 3 dB variation on the field strength amplitude (or a reflectivity level of – 10 dB) at 100 MHz for omnidirectional radiating devices, and better than ±0.1 dB variation above 900 MHz for moderately directive antennas under test, i.e. a reflectivity level of – 45 dB. In order to fulfil these requirements the end walls of the room had to be covered by 450 mm long absorbers, and the side walls, floor and ceiling of the room by 910 mm long absorbers.

Firstly, measurements were done with a wideband dipole and a wideband double-ridged horn at 1.6 - 3 GHz. The antennas were placed 1.12 – 1.47 m apart, in 50 mm steps. The results show that the performance stays slightly below these specifications, namely with overall field variations of about ± 0.25 dB (peak to peak). At around 2 - 2.2 GHz, i.e. at the resonance frequency of the wideband dipole, the field homogeneity is slightly better with ± 0.15 dB while at around 2.4 - 2.7 GHz the fields are least homogeneous with fluctuations of up to ± 0.8 dB. This was probably due to the preliminary fixture of the measurement antenna and the cables, which were not yet optimised for low field interference. An improvement of the field homogeneity is expected after the installation of a positioning system with two rotators on two perpendicular axes which allows automated measurements of three-dimensional radiation patterns (see Figure 8 (r.)). This system will allow the radiation pattern measurement of a mobile handset together with the head model of a human user.

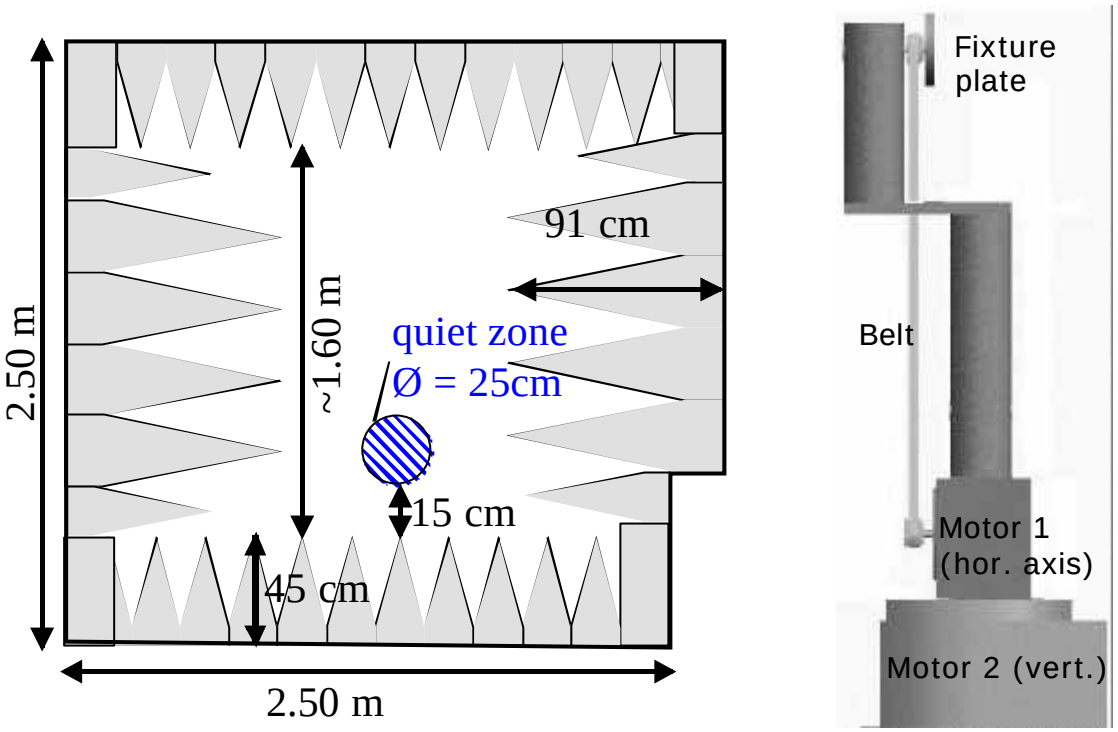

Figure 8: Design of small anechoic chamber at IRC, with 2.5 m long and 2.4 m high side walls (l.). Automated positioning system with a vertical and a horizontal axis, the latter driven via a belt (r.).

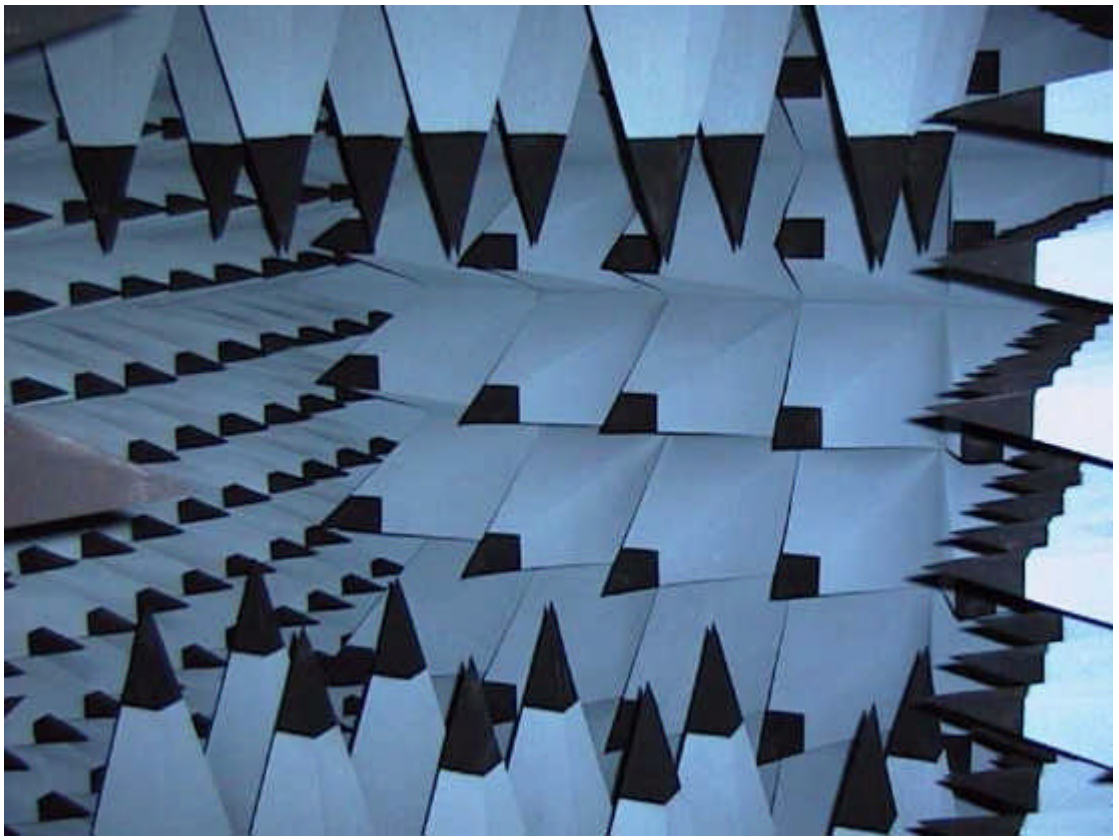

Figure 9: Photo of the absorber lining in the small anechoic chamber at IRC, one side panel open, looking at the opposite, fixed sidewall with 900 mm long absorbers. Also

ceiling and floor are lined with 900 mm long absorbers, and other walls with 450 mm long absorbers.

3.4. Quarter-wave cap: a means for decreasing the influence of cables

Another major problem often encountered when performing antenna measurements especially with small antennas in whichever size of chamber, is the influence of the involved cables on the radiation characteristics. In the calibration of antennas according to standard methods, a measurement of the complex transmission and reflection coefficient with the antenna under test (AUT) and a well known measurement antenna must be performed. Therefore, a coaxial cable must be used to connect the AUT and a network analyser. This situation does not resemble the standard operation situation, especially for portable communications equipment. The signal being measured or transmitted by the AUT will induce RF currents on the exterior of the connected coaxial feed cable.

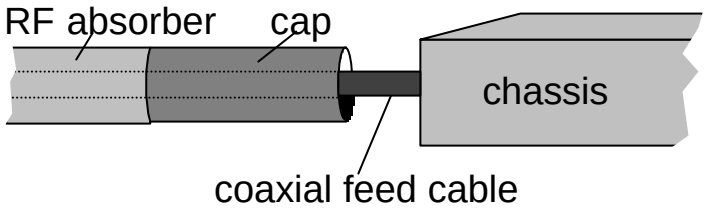

Figure 10: Attaching a cap with the open end towards handset-antenna combination, simulating an open end by providing a narrow-band trap for surface currents.

This is caused by two distinct effects: Firstly, the conducting cable is placed in the reactive near field of the antenna. This will change the resistive and reactive parts of the input impedance, i.e. the matching, and hereby changes the radiation characteristics of the antenna itself. Secondly, the imperfect balance between antenna and chassis will cause currents to leak from the chassis to the outside of the connected cable. This causes the cable itself to act as a radiator. Both effects can change the measured radiation characteristic of the antenna severely, as has been shown in [21] and [22] for the case of larger antennas. The effect is especially strong, when the cable is situated parallel to the polarisation of the antenna. While the effect can be somewhat controlled during measurements of large antennas, it is much more difficult to suppress the influence of a feed cable on the radiation of a small antenna. This is due to the fact that a smaller antenna usually has a lower directivity. While large, directive antennas can have the feeding cable simply attached in the direction of their radiation minimum, i.e. generally in their back lobe, a small antenna will always interact more with the feeding cable as it can not be placed in any minimum. Also, small antennas are generally imperfectly balanced dipoles, or patches with a small ground plane, where the chassis acts like a ground plane. Those antennas will be affected more easily by a conducting cable attached to the chassis than a larger horn antenna or a log-periodic antenna consisting of matched dipole antennas.

A new method proposed here is to simulate an open termination for the energy propagating on the surface of the feed cable. This is possible by placing a coaxial cap with a length of about a quarter of a wavelength on the outside of the feed cable which works as a trap to waves propagating on the shield of the cable (Figure 10). Especially at higher frequencies a cap is

much easier to implement than e.g. ferrite chokes, because suitable ferrite materials with a high permeability and low losses are difficult to produce for frequencies around and above 1 GHz.

Computer simulation were done in [P4] for a handset with the dimensions $h \times w \times t = 100 \times 40 \times 10$ mm^3 plus a l_a = 20 mm long, dielectrically loaded monopole antenna (see Fig. 11), resonant at 1 GHz and placed at a typical position on the handset. A 160 mm long metal stub was attached to the bottom of the chassis to imitate the effect of a coaxial feed cable. Then, a ferrite bead (length 80 mm, diameter 20 mm) was placed around the cable. The ferrite had a relative permittivity ε_r' = 50, a relative permeability μ_r' = 50, and electric and magnetic loss tangents of 0.1. In several more simulations 60 – 65 mm long caps with diameters of 16 – 20 mm were placed on the cable. The gap between the handset bottom and the open-end of the cap was 10 – 20 mm. Thus, the effective distance between handset and the closed end of the cap was about quarter of the wavelength at 1 GHz. The results show that with such a cap the radiation pattern is much closer to the original radiation pattern than if ferrite beads are used to suppress the currents on the outer shield of the feed cable (see Table 3). In case ferrites are used to block the currents, the error in the pattern is lower than with just a cable, but the ferrites absorb much of the energy, the total radiated power was decreased by almost 2 dB. It can also be seen that the performance of the cap is not very sensitive to the length and diameter of the cap or its distance from the handset. The bandwidth of this cap can be expected to be generally better than ±5 % (see Table 4) thereby enabling measurements over a typical bandwidth of mobile handset.

Table 3: Two figures of merit - total radiated power and average of differences in the far-field pattern in the E-plane - compared to the reference case. *f* = 1 GHz.

Case description (length,distance,[mm])	$P_{rad,tot}$ [dBm]	ave$\lvert\Delta E_{far}$[dB]$\rvert$ [dB]
handset alone (ref.)	28.7	0
160 mm feed cable	28.6	3.29
ferrite bead (80, 30)	26.9	2.80
cap 1 (60, 15)	28.7	1.41
cap 2 (60, 20)	28.9	1.04
cap 3 (65, 10)	28.6	1.63
cap 4 (60, 15, ∅=20)	28.8	1.87

Table 4: Figures of merit for two cases at 1.05 GHz.

Cases (l.,dist.,[mm])	$\lvert\Delta(P_{rad,tot}$[dBm]$)\rvert$ [dB]	ave$\lvert\Delta(E_{far}$[dB]$)\rvert$ [dB]
cap 1 (60, 15)	0.25	1.07
cap 3 (65, 10)	0.54	2.38

In Fig. 12 and 13 the performance of the two different measures against surface currents on the feed cable is illustrated with help of the E-plan radiation patterns. It can clearly be seen, how the radiation pattern of the handset is affected by the attached cable stub, and how the ferrite bead, and in a better manner the cap of different dimensions, results in a radiation pattern close to the original one.

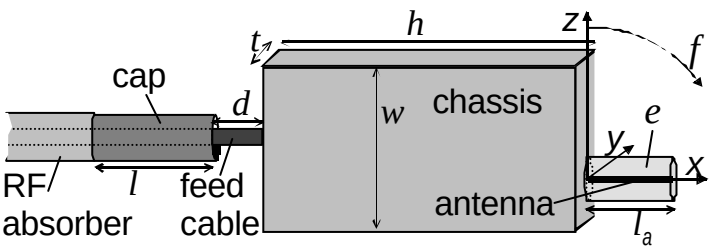

Figure 11: Dimensions of simulated handset with a cable and cap (open end towards handset) attached, coordinate system and visualisation of E-plane.

$$\frac{P_{rr}}{P_{in}} = \frac{r_1 A_1 \cdot r_2 A_2}{(\lambda d)^2}$$

Figure 12: Simulated E-plane radiation pattern at 1 GHz: $|E|$ at 1 m distance, handset alone (solid), handset with 2.4 mm thick, 160 mm long cable (dashed), and a 80 mm long, 20 mm thick ferrite (ε_r=50-j5, μ_r=50-j5) attached to cable at 30 mm distance (dotted).

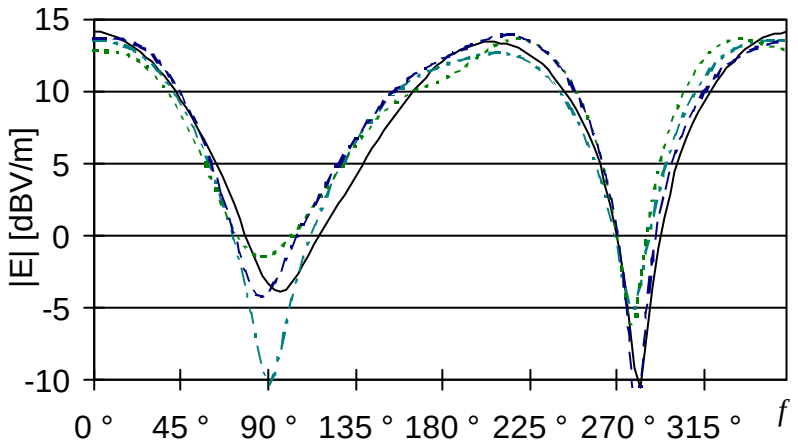

Figure 13: Simulated E-plane radiation pattern at 1 GHz: $|E|$ at 1 m distance, handset alone (solid), handset with 2.4 mm thick, 160 mm long cable plus cap 1 (length 60 mm, distance 15 mm, dash-dot), cap 2 (l = 60 mm, d = 20 mm, dashed), and cap 3 (l = 65 mm, d = 10 mm, dotted).

4. Computer simulations and the prediction of radiated EMI

At the end of the design process of a new electronic equipment, there is always the requirement to perform a final test for electromagnetic compatibility (EMC) of the device. This includes the conducted and radiated electromagnetic interference (EMI) the device causes as well as on its part the susceptibility to external sources of EMI. Tests for radiated EMI according to present standards are performed on open area test sites or in the low-cost alternative GTEM cells as was discussed above.

Even so, the GTEM cell with its small size and relatively straight forward measurement procedure is still a relatively costly equipment to use it for quick, preliminary tests of radiated EMC during the design phase of a new electronic product. Preliminary tests of new equipment are getting more and more important as the product cycles are getting shorter and shorter, which leads to high additional costs if a device needs to be redesigned after failing the final EMC tests. In order to provide faster, more cost effective methods of pre-compliance testing, the last part of the thesis concentrates on the definition of a new procedure using EM field simulation software for predicting radiation characteristics of small electronic devices in terms of EMC. As opposed to measurements, computer simulations need no prototype of a device. EM fields software can also be used to simulate a device together with several possible shielding enclosures, which can have large effects on the common mode radiation from e.g. I/O cables attached to the device. Therefore, computer simulations as a new method for predicting radiated EMI of small electronic devices are presented and evaluated. Reference measurements have been done to validate the results.

4.1. Available field simulation tools suitable for predicting radiated EMI

There are different approaches to the prediction of radiated EMI from equipment. First there are expert systems which do a qualitative analysis of the layout and structure of a device [23]. Then there are software packages, that calculate the actual field strength at a certain distance, based on the model of the circuit board in terms of its dimensions and materials on the one hand, and the current distribution (i.e. the RF signals) in the circuit. Some of these tools can import an existing PCB layout to streamline the process of EMI prediction [24]. This often coincides with the usage of the Method of Moments (MoM) for the EM field calculation. Other methods like the Finite Difference Time Domain (FDTD) method are more suitable when the presence of dielectric material and enclosures is relevant for the EMI analysis [25].

After gathering a list of available commercial computer simulation tool for 3D EM field analysis available on the market, a list of pros and contras was made and evaluated (Table 5). Finally, Maxwell Eminence (Ansoft) and EMC Workbench (Incases) were chosen for further evaluation with two test circuits. Maxwell Eminence was chosen for its ability to model dielectric materials as well as ferrites, which is useful when modelling whole equipment with possible non-metallic elements or enclosures. EMC Workbench offers the import of circuit board layout files which is useful when analysing more complex circuits.

Table 5: List of five software packages considered most suitable for simulating radiated fields of printed circuit boards, or small electronic devices in general.

3D-field solvers	**HFSS**	**Maxwell Eminence**	**MAFIA**	**EMC-Workbench**	**IE3D**
provider	Hewlett Packard	Ansoft	CST	Incases	Zeland
platform	UNIX/PC	UNIX/PC	UNIX	UNIX/PC	PC
method	FEM	FEM	FIM (TD)	MOM	MOM
input	GUI	GUI	GUI	ASCII	GUI
imports	-	Pro-E, Unigraph.	CAD	CAD, Spice, Pads, Mentor	Touchstone, GDSII
models	wires, dielectrics of any shape, also anisotropic, antenna arrays	wires, dielectrics of any shape, also anisotropic, antenna arrays	wires, dielectrics of any shape, lumped elements	PCB tracks and circuit elements (macro models), enclosures, no dielectrics	lossy & anisotropic materials lumped elements (S parameters)
excitation	TL input ports multiple ports voltage gap plane wave	voltage and current source, plane wave, eddy current solver	voltage source plane wave sub grids	voltage and current source	current sources TL ports
calculates	radiation pattern energy density surface currents S-parameters TL-parameters	radiation pattern energy density S-parameters TL-parameters forces	radiation pattern energy density TL eigen modes S-parameters	radiation pattern current density crosstalk signal integrity	radiation pattern near fields current density polarised fields s-parameters
output	function plots smith charts arrow, contour & shaded plots, 3Dfar-field plots animations	function plots arrow, contour & shaded plots, animations	function plots arrow, contour & shaded plots 3Dfar field plots	contour plots arrow plots near field scans radiation pattern 3Dfar-field plots	function plots contour plots 3Dfar-field plots

4.2. Simulation of two test structures and analysis of results

Computer simulations with the Maxwell Eminence package employing the Finite Element Method (FEM) were applied to a magnetic field generator (Fig. 14) at a frequency range of 30 to 500 MHz. The maximum far field at 10 m distance for a constant loop current was calculated. In parallel, circuit simulations determined the actual current spectrum of the loop. These were then used to scale the calculated maximum far field to the correct level at each frequency point. The predicted values were compared to far field measurements done with the field generator in an anechoic chamber at 4.4 m distance. Depending on the frequency, predicted and measured values show differences from a few to 15 dB [P5]. Field calculations at 28 frequency points between 30 and 500 MHz took about 100 hours on a typical UNIX workstation.

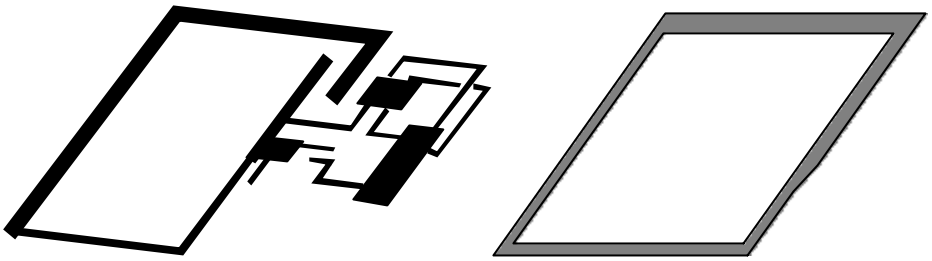

Figure 14: Original layout of magnetic field generator (left) and simplified loop model (right) for numerical far-field computation

Secondly, the same FEM package, as well as the Method of Moments (MoM) software package EMC-Workbench (Incases) were applied to the radiation calculation of a switched mode power supply (SMPS). As the possibility to simulate complex structures is quite limited the calculation model of the power supply consisted merely of the traces that carried the largest currents during operation and were therefore most likely sources for EMI. The simulation model of the traces was very close to the actual geometry of the involved current traces on the PCB (see Fig. 15 and 16). An ideal current source was inserted at the position of the active element with a constant current for all frequencies.

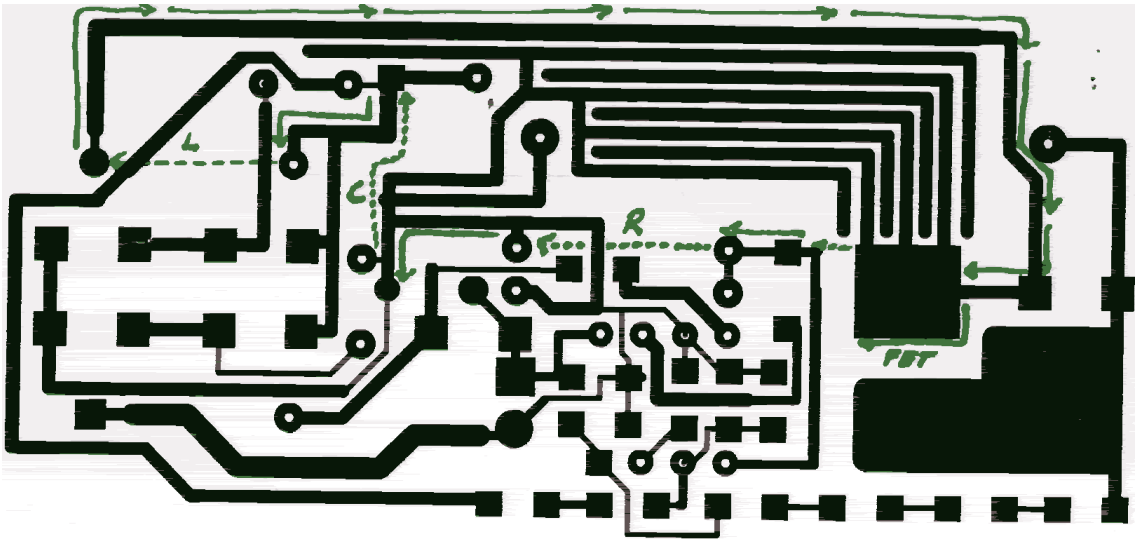

Figure 15: Illustrating the relevant current trace when the FET is active.

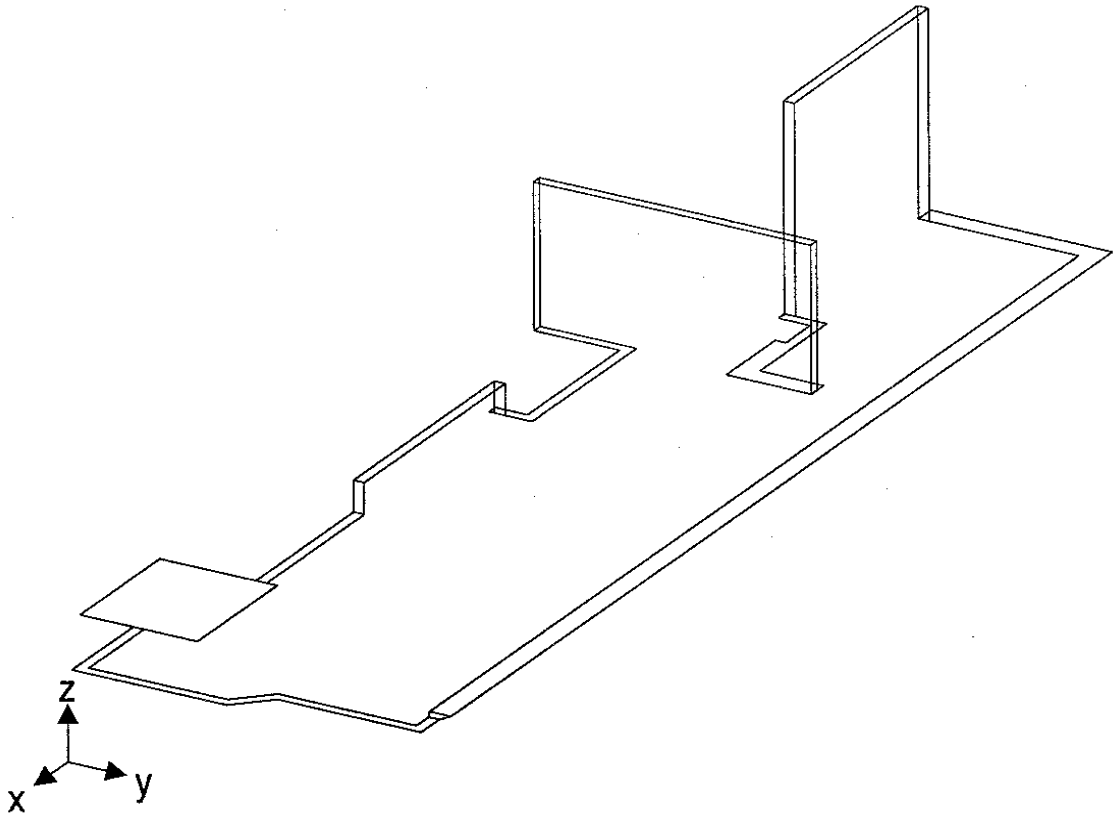

Figure 16: Model of current trace for far-field calculations in Maxwell Eminence and EMC Workbench.

The circuit contained two loops with an area of 12 cm^2 through which the switched current flows alternatively. The switching period t_s = 5 µs (Fig. 17). The switching is performed by a field-effect transistor (FET) in combination with a diode. The switching that is otherwise impossible to simulate straight forward can be handled in the frequency domain by adding the complex field values of the two separately calculated loops during post processing, before determining the maximum field strength. The calculation time of the FEM package was 200 hours for 28 frequency points. The MoM package on the other hand showed a much faster calculation time (in the order of minutes) while both FEM and MoM predicted the radiation in the same order of magnitude. The MoM software package does however not allow the modelling of dielectric materials or ferrites which might limit its application in some cases. FEM allows the modelling of dielectric and lossy materials.

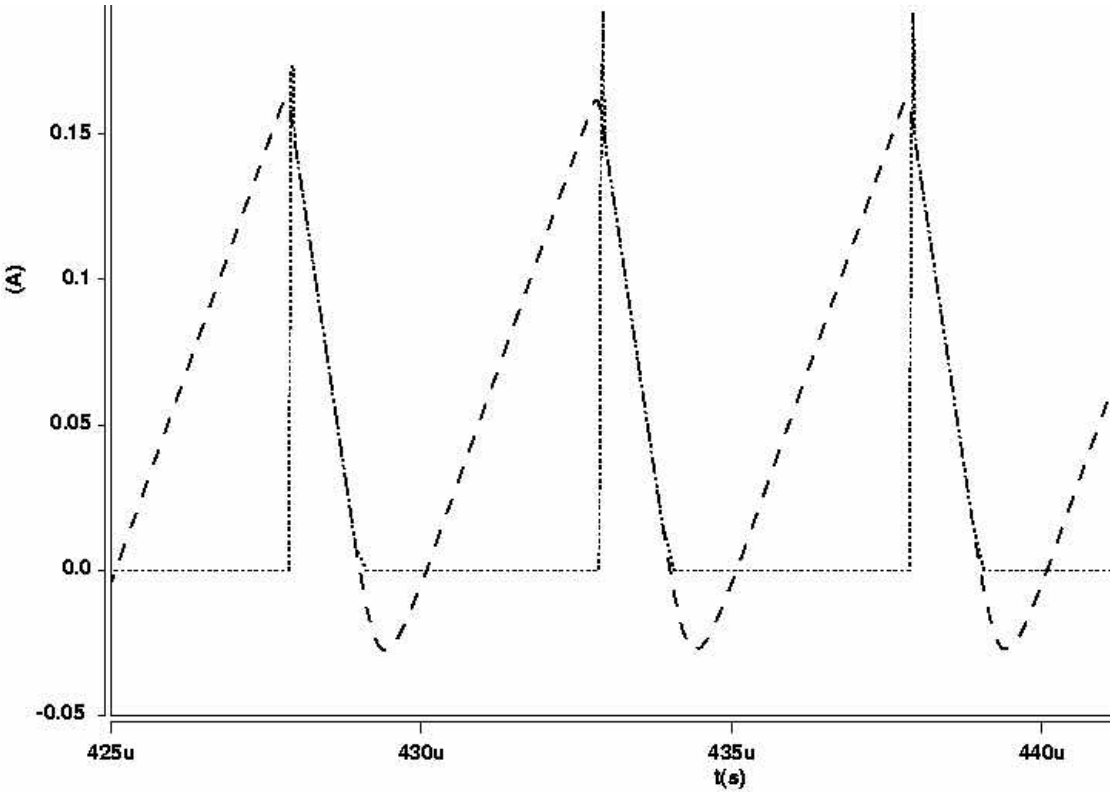

Figure 17: Time domain presentation of the currents through the two main traces on the PCB, when the diode is conducting (dashed) and when the FET is active (dotted).

In parallel, the current spectrum in each of the two loop traces was calculated in a circuit simulation software (Fig. 18). The spectrum was used to scale down the results of the simulated maximum field strength. The final maximum field strength calculated with the two methods was compared to the field strength measured in a GTEM cell (Fig. 19). At frequencies from 30 – 330 MHz the predictions by the two software packages agree within ± 5 dB with the GTEM cell reference measurement. At higher frequencies the simulated far field increases, in the case of EMC-Workbench by several 10 dB above the measured values. The reason for this could not yet be identified. However, at lower frequencies, where SMPSs usually produce EMI problems, the results show the usefulness of simulations for EMI prediction.

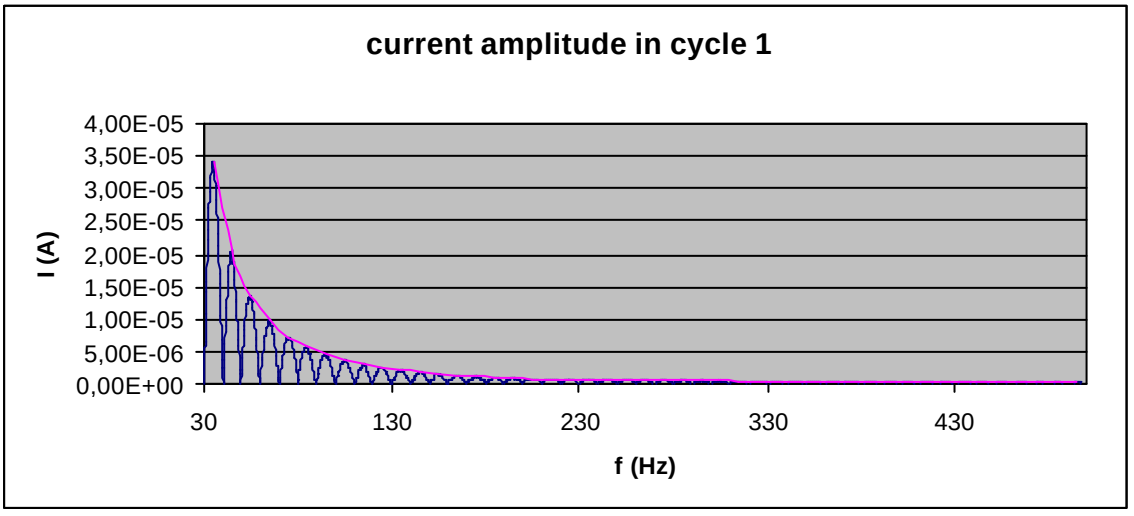

Figure 18: Simulated current spectrum of the FET trace calculated by circuit simulator software Saber.

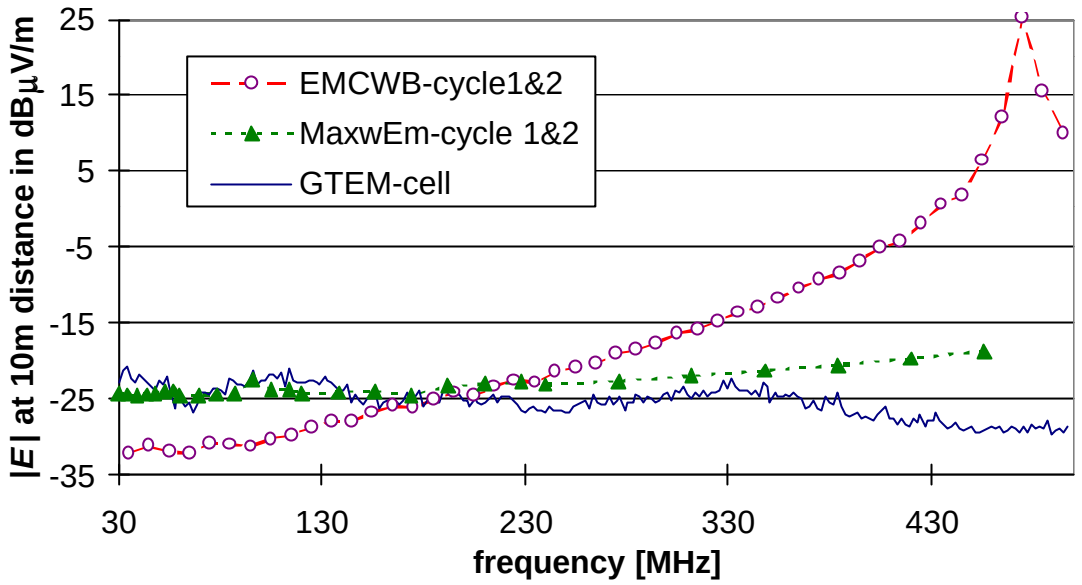

Figure 19: E-field at 10m distance simulated with EMC-WB and Maxwell Eminence compared to radiation prediction at 10m, based on GTEM cell measurement. (The simulated resonance at 460 MHz could not yet be explained).

Simulations prove to be a promising means of pre-evaluating the EMI of a device, especially as they can be used already very early in the design process. Other software packages like MAFIA (CST) should be investigated in a similar matter to evaluate possible advantages of a time domain method. The possible complexity of the models when including cables attached to a circuit and shielding enclosures is also still a subject for further investigation.

5. Conclusions

The aim of this work was to develop and describe new measurement methods for the determination of the direction- and frequency-dependent RF radiation characteristics of small radiating devices. This is an important subject in research in the field of radio engineering at frequencies from 30 MHz up to 5 GHz, as e.g. in the area of future mobile communication systems, the behaviour of the antennas in their working environment must be well known before a new mobile handset can be designed.

The use of large anechoic chambers seems unreasonably expensive for quick test of an antenna, and also for final calibration measurements. The feasibility of using a GTEM cell or small anechoic chambers for small antenna measurements have been investigated by both measurements and 3D field simulations.

It has been found that up to 1-2 GHz a medium sized GTEM cell can be used to measure certain characteristics of the radiation patterns of small antennas, such as the 3 dB-beamwidth and the polarisation, as well as - within the limits of the dynamic range of the GTEM cell - the directivity of a small antenna. The results also indicate the GTEM cell be suitable for efficiency measurements, i.e. the determination of the total radiated power of a small antenna.

The use of small anechoic chambers for small antenna measurements has been found suitable at frequencies around 1 – 2 GHz, both by measurements and computer simulations. As recommendations for the size of the chamber a distance between the AUT and the measurement antenna of 1 m, and a distance between AUT and RF absorber lining on the walls of 15 – 20 cm is recommended. With that small distances it will be possible to construct table-top sized, portable anechoic chambers that can be used for quick antenna measurements, including the measurements of the radiation pattern, directivity and efficiency of a small antenna, with the same accuracy that is otherwise reached only in large anechoic chambers.

The electrically small size of the handset makes mobile communications antennas very sensitive to measurement cables used in antenna measurements of their 3-dimensional antenna pattern with complex field strength and two polarisations. A new method has been developed that suppresses the influence of the cables connecting the network analyser and the AUT, e.g. during radiation pattern measurements of new mobile communications antennas, usually mounted on a handset. A quarter-wave long cap close to the AUT or handset acts like an open end that reflects all surface currents on the cable. Without any measures the currents on the cable would change the current distribution on the handset and thus the radiation pattern of the handset considerably, when compared to its normal mode of operation where it will be situated isolated in free space or close to a large lossy body - the human user. A conventional measure against the surface currents on the feed cable would be ferrite beads placed around the cable relatively close to the handset. In computer simulations the suppression of the currents on the cable has been less successful with ferrites than with help of the new quarter-wave cap method.

The last part of the thesis concentrates on the development and evaluation of new, low-cost methods of pre-compliance testing. Standard tests of the radiated EMC can be performed e.g. on an OATS. Even though alternative closed chambers such as the GTEM cell are nowadays used in standard EMC tests measurement procedures are still a relatively costly equipment to use it for quick, preliminary tests of radiated EMC during the design phase of a new electronic product.

Preliminary EMC tests, so-called pre-compliance tests, for new products become increasingly important because product cycles are getting shorter and shorter. The failure in final EMC tests means high losses. This has to be avoided by analysing and testing the EMC behaviour during the design of a new product. Computer simulations are presented as a good and useful method for predicting radiated EMI of small electronic devices, because they need no prototype of a device. Also, a device can be simulated together with several possible shielding enclosures in order to find the optimum solution.

6. Summary of the publications

In the first paper [P1] the applicability of the GTEM cell in small antenna measurements was studied. It is shown that up to 2 GHz the field homogeneity in the testing volume of the cell is sufficient to perform radiation pattern measurements, limited only by the dynamic range of the cell which is about 20 dB due to the imperfect termination of the cell. The polarisation isolation of the GTEM cell is good and allows polarisation measurements.

The second paper [P2] discusses the effect that the absorbers of an anechoic chamber have on an antenna, if they reach into the vicinity of the antenna. Measurements revealed that at 1 GHz a distance of 100 mm between antenna and absorbers is sufficient to be able to neglect the reflected fields from the absorbers during radiation pattern measurements. Also a very narrow transmission channel of just 100 mm formed by the side wall of the anechoic chamber would be sufficient to ensure an unchanged transmission between the antennas.

The third paper [P3] relates to computer simulations to investigate the effect of absorbers in the vicinity of an antenna. Again it was shown that at a distance of 100 mm the interference pattern between direct and reflected field can be expected to be close to the direct pattern, closer than 0.1 dB in the main lobe.

In the fourth paper [P4] a new method was introduced that eliminates the effect of cables connecting a network analyser to a small antenna on radiation characteristics of the antenna during calibration measurements. Often, ferrite beads are used to suppress and partly absorb the currents on the outer of the cable. Nevertheless, the current distribution on the antenna or handset is changed compared to the normal mode of operation. More promising is a quarter wave cap situated around the cable, short cut to the outer conductor of the cable on one end, and the open side towards the small antenna. The cap acts like an open end and thereby reflects the currents flowing on the outer of the cable. The original radiation pattern of the small antenna is hereby mostly preserved.

The fifth paper [P5] is a summary of the evaluation of two new methods for pre-compliance test in EMC. One is a near-field method that has been developed by co-author T. Laitinen. The second method is based on computer simulations to predict the radiated EMI from a simplified model of a switched mode power supply. It was shown that the computer simulations compared to far-field measurements could predict the radiation within 15 dB, which is enough to reveal future EMC problems already early in the design phase of a new device.

7. References

[1] "IEEE Standard Test Procedures for Antennas," *ANSI/IEEE Std. 149-1979*, IEEE Press, New York, NY, 1980, 143 pages.

[2] "Limits and Methods of Measurement of Radio Interference Characteristics of Information Technology Equipment," International Electrotechnical Commission, International Special Committee on Radio Interference, *European standard EN 55 022 (eq. CISPR 22)*, Brussels, 1998, 107 p.

[3] "Methods of measurement of disturbances and immunity," *CISPR 16-2*, International Electrotechnical commission, First edition 1996-11, Specification for radio disturbance and immunity measuring apparatus and methods, Part 2, 151 p.

[4] "Interference relating to information technology equipment," *CISPR /G/135/INF*, International Electrotechnical commission, 1997-11, Sub-Committee G, 16p.

[5] D. Königstein, D. Hansen, "A New Family of TEM-cells with Enlarged Bandwidth and Optimized Working Volume," *Proceedings of the 7th International Zurich Symposium on Electromagnetic Compatibility*, Zurich, March, 1987, pp. 127 - 132.

[6] D. Hansen, D. Königstein, "Vorrichtung zur EMI-Prüfung elektronischer Geräte," *Patentschrift bei der Schweizerischen Eidgenossenschaft*, CH 670 174 A5, May, 1989, 5 p.

[7] "Electromagnetic Compatibility (EMC) - Part 4: Testing and Measurement Techniques - Section 3: Radiated, Radio-Frequency, Electromagnetic Field Immunity Test," *International Standard CEI/IEC 1000-4-3 (EN 61000-4-3)*, Geneva, Edition 1.1; Edition 1: 1995 Consolidated with Amendment 1: 1998, 73 p.

[8] S.R. Mishra, S. Kashyap, R. Balaberda, "Input Impedance of Antennas inside Enclosures," *Proceedings of the 1985 IEEE International Symposium on Electromagnetic Compatibility*, Wakefield, MA, USA, August 1985, pp. 534 - 538.

[9] S. Hawlitschka, W. Graf, P. Guidi, H.U. Schmidt, "Untersuchungen des Abstrahlverhaltens von Antennen und Störstrahlern in TEM-Wellenleitern," *Digest of the 5th International Fair and Congress for Electromagnetic Compatibility*, Karlsruhe, Germany, February, 1996, pp. 301 - 308.

[10] E. L. Bronaugh, J.D.M.Osburn, "Measuring Antenna Parameters in a GHz Transverse Electromagnetic (GTEM) Cell," *Proceedings of the 1992 IEEE AP-S International Symposium, URSI, & NEM*, Chicago, IL, July, 1992, pp. 2064 - 2066.

[11] R. De Leo, T. Rozzi, C. Svara, L. Zappelli, "Rigorous analysis of the GTEM cell," *IEEE Transactions on Microwave Theory and Techniques*, Vol.39, No.3, March, 1991, pp. 488 - 499.

[12] C. Icheln, *'The construction and application of a GTEM cell'*, Diploma Thesis at the University of Technology Hamburg-Harburg, Nov. 1995, 53 p.

[13] A.P. Duffy, A.J.M. Williams, "Optimising Mode Stirred Chambers", *Proceedings of the 13th International Zurich Symposium on EMC*, Zurich, Switzerland, February, 1999, pp. 685 - 688.

[14] R. H. Johnston, J. G. McRory, "An improved Small Antenna Radiation-Efficiency Measurement Method," *Antennas and Propagation Magazine*, Vol. 40, No. 5, October, 1998, pp. 40 - 48.

[15] M. Klingler, J. Rioult, J-P. Ghys, S. Ficheux, "Wideband Total Radiated Power Measurements of Electronic Equipment in TEM and GTEM Cells", *Proceedings of the 13th International Zurich Symposium on EMC*, Zurich, Switzerland, February, 1999, pp. 665 - 670.

[16] D. Green, D. Smith, "Design, construction and performance of a small, low cost anechoic measuring system for research applications," *Proceedings of the 1995 IEEE AP-S International Symposium*, Newport Beach, California, June, 1995, pp. 1738 - 1741.

[17] C.A. Balanis, Antenna Theory, Analysis and Design, 2nd Edition, John Wiley & Sons, 1997, 790 p.

[18] T. Macnamara, *Handbook of Antennas for EMC*, Artech House, Sept. 1995, 275 p.

[19] J.D. Kraus, Antennas, 2nd Edition, New York, McGraw-Hill Book Company, March 1988, 892 p.

[20] J.S. Hollis, T.J. Lyon, L. Clayton, *Microwave Antenna Measurements*, 2nd ed., Scientific Atlanta, July, 1970, p. 14-10.

[21] J. DeMarinis, "The Antenna Cable as a Source of Error in EMI Measurements," *Proceedings of the 1988 IEEE International Symposium on EMC*, Seattle, Washington, August 1988, pp. 9 - 14.

[22] S. Saario, D.V. Thiel, J.W. Lu, S.G. O'Keefe, "An assessment of cable radiation effects on mobile communications antenna measurements," *Proceedings of the 1997 IEEE International Symposium on Antennas and Propagation*, Montreal, Canada, July, 1997, pp. 550 - 553.

[23] N. Kashyap, T. Hubing, J. Drewniak, T. Van Doren, "An expert system for predicting radiated EMI from PCB's", *Proceedings of the IEEE 1997 International Symposium on Electromagnetic Compatibility*, August, 1997, pp. 444 - 449.

[24] P.K. Saha, J. Dowling, “Reliable prediction of EM radiation from a PCB at the design stage of electronic equipment”, *IEEE Transactions on Electromagnetic Compatibility*, vol. 40, no. 2, pp. 166 -174.

[25] D.M. Hockanson, J.L. Drewniak, T.H. Hubing, T.P. Van Doren, “FDTD modeling of thin wires for simulating common-mode radiation from structures with attached cables”, *Symposium Record of the 1995 IEEE International Symposium on Electromagnetic Compatibility*, August, 1995, pp. 168 - 173.